NRL Report 5643

ATMOSPHERIC ATTENUATION COEFFICIENTS IN THE VISIBLE AND INFRARED REGIONS

C. L. Knestrick, T. H. Cosden,
and J. A. Curcio

Radiometry Branch
Optics Division

August 8, 1961

CONTENTS

ABSTRACT

Atmospheric spectral attenuation coefficients have been measured in ten narrow wavelength bands between 0.4 and 2.3 microns for a variety of weather conditions using two overwater, sea-level paths of 5.5 km and 16.3 km. The wavelengths bands were chosen so as to avoid molecular absorption and were isolated by interference filters. A 60-inch-diameter, high-intensity source and a 24-inch-diameter, narrow-field receiver were combined to yield relative scattering attenuation coefficients (σ) as a function of wavelength (λ). These were then scaled using values obtained at one wavelength with a visual telephotometer. Log σ vs log λ curves show a wide range of slopes and shapes, with a tendency toward less slope in the infrared (indicating that σ is becoming independent of λ in the infrared). Some correlation with relative humidity was found for relative humidities greater than 70 percent. The anomalous slope reversal between 1.68 and 2.27μ is discussed, and a possible explanation for the reversal is given as selective scattering by the aerosol at these wavelengths.

PROBLEM STATUS

This is a final report on one phase of this problem; work is continuing on other phases.

AUTHORIZATION

NRL Problem A02-17
Project RR 004-02-41-5152

Manuscript submitted May 22, 1961.

ATMOSPHERIC ATTENUATION COEFFICIENTS IN THE VISIBLE AND INFRARED REGIONS

INTRODUCTION

Radiation passing through the atmosphere is subject to attenuation by molecular and particulate scattering and by absorption. The absorption is caused by permanent gases and water vapor and occurs predominately at discrete wavelengths. Scattering on the other hand is more continuous with wavelength and occurs to some extent at all wavelengths in the visible and near-infrared regions of the spectrum. Therefore, by isolating narrow wavelength intervals between absorption bands one can measure the effect of scattering with relative freedom from absorption influences.

PROCEDURE

Atmospheric spectral attenuation coefficients of the horizontal atmosphere were measured in ten narrow wavelength bands between 0.4 and 2.3 microns (μ) through the use of interference filters which isolated the different bands. The wavelengths were chosen to be as free as possible from known molecular absorption. Two different over-water paths were used in the Chesapeake Bay area, a 5.5-km path which was nearly parallel to the shoreline and a 16.3-km path which was entirely over water. The period covered by this series of measurements extended from April 1959 to January 1960 and included cases of light fog, haze, and clear weather. The 2 percent transmission range* (at 0.67μ) encountered over the 5.5-km path varied from 5.5 km to 72 km and over the 16.3-km path it varied from 37 km to 97 km. Relative humidities varied from 36 percent to 100 percent.

The light source was a xenon flash lamp (FT-503) installed at the focus of a 60-inch-diameter reflector. The receiver consisted of an f/3.5 front-surfaced collector mirror, 24 inches in diameter, and a Newtonian diagonal mirror which was used to deflect the beam to a 2-inch-square, uncooled, lead-sulfide photodetector (Fig. 1). The filters were inserted in the focal plane of the mirror, and the detector was mounted behind the focus. The output of the detector was displayed on an oscilloscope screen on which were read peak deflections from the lamp pulses, which occurred at 30-second intervals. Relative transmission values were obtained by comparing the signals received at each wavelength over 5.5 or 16.3 km to the corresponding signals received on a "zero" (zero attenuation) run. During a zero run an attenuation disk with radial slots was placed over the collector to compensate for the signal increase caused by bringing the source close to the receiver. A 1000-ft path was used for the zero runs, which were made only when the meteorological range was greater than 32 km.

CALIBRATION

Method

The transmission of the atmosphere at 0.67μ was measured using a visual telephotometer for the Koschmieder method of contrast measurement, as described by Curcio and Durbin (1). The telephotometer consisted of a standard red-filtered Leeds and Northrop

*This is the range over which the atmospheric transmittance is 2 percent.

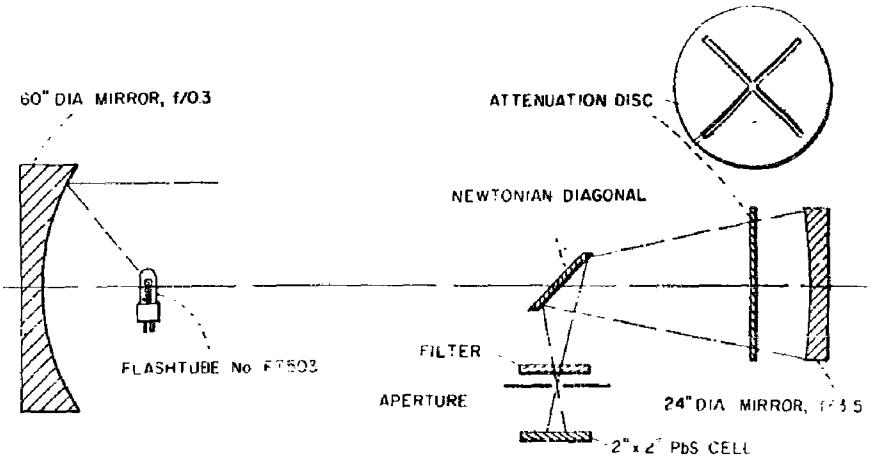

Fig. 1 - Source-receiver system
(attenuation disk used for zero runs only)

optical brightness pyrometer fitted with a telescopic lens. It was used to measure the brightness of a distant dark object, such as pine woods, and of the sky horizon. By converting the brightness temperature readings of both objects to spectral radiant emittances and substituting in the Koschmieder relationship, one obtains the transmission at 0.67μ to the woods (1). The transmission value at 0.67μ was used to scale the photoelectric relative transmission curve to one of absolute transmission. The absolute transmission values were then converted to attenuation coefficients for a 1-km path. At this stage, the coefficients were plotted vs wavelength and were then replotted after a subtraction of the computed contribution due to Rayleigh scattering from air molecules.

Filters

A composite curve of transmittance vs wavelength for all the filters used is shown in Fig. 2. In the visible region the bandwidths at half peak transmittance average about 140 A (14 mμ) for nearly parallel light. The filters for 1.6 and 2.2μ have half bandwidths of the order of 100 mμ. Since the filters were used in converging light, the bandwidths in practice were greater than the figure indicates. From measurements of spectral transmittance vs angle of incidence it was found that the transmittance curve shifted 6 mμ for one of the visible filters and 3 mμ for the 1.6μ filter for an incidence or convergence angle of 8 degrees. The total average bandwidth at half peak transmittance then becomes 20 mμ for the visible region and still of the order of 100 mμ for the infrared. The peak wavelengths of the two infrared filters are not quite centered between the water-vapor absorption bands but are located slightly on the long wavelength side of center, resulting in an effective shift of this side of the filter pass band dependent upon water content of the atmosphere. The data at these points were corrected for this effect using the Passman and Larmore (2) values for transmission as a function of water content.

Methane

When the attenuation values at 2.27μ seemed to be consistently high we investigated the possibility of absorption by other gases in the atmosphere and found that Migeotte (3) lists several methane bands in this region: namely, at 2.20, 2.32, 2.37, and 2.43μ. Accordingly, the transmissivity of methane was measured in the laboratory using the PbS cell and filter combination. It was found that 1 atm-cm of methane, which was equivalent to that which would frequently be encountered in a 5.5-km path, had an effective transmittance of 97 percent and the transmittance for a 15.3-km equivalent path was 91 percent.

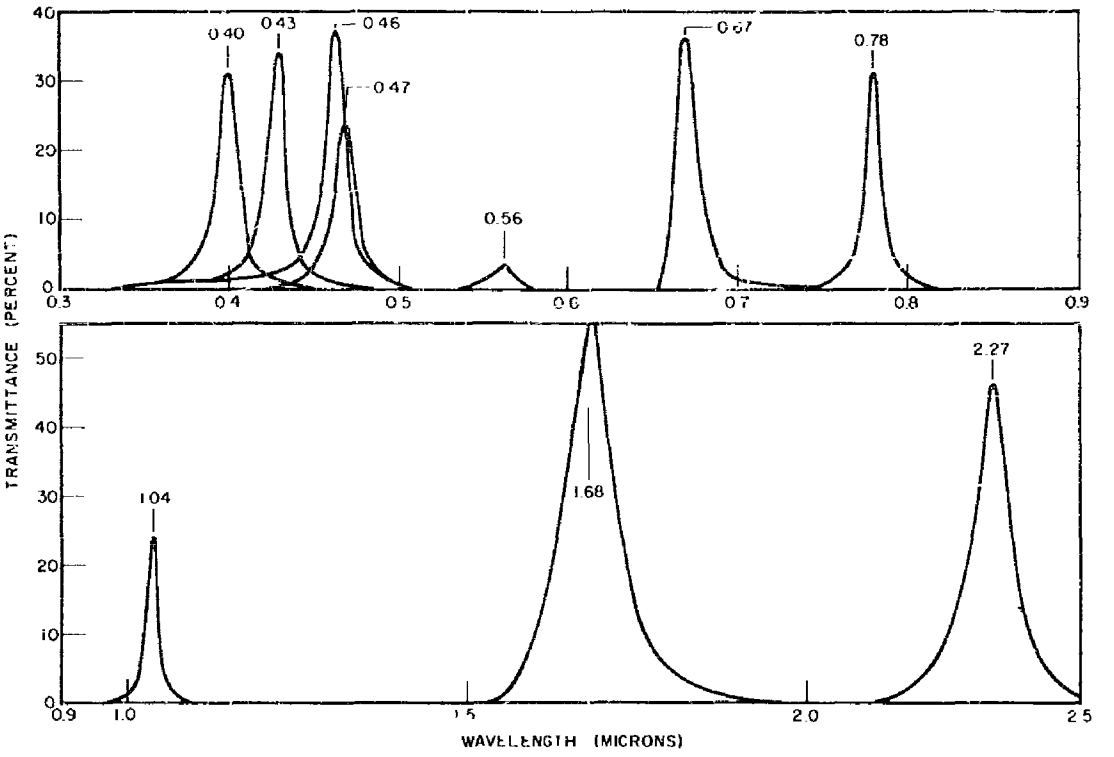

Fig. 2 - Composite transmittance curve for filters used to measure attenuation coefficients

The amounts of methane in the two paths were calculated using the ARDC model atmosphere figure of 1.4 parts per million of methane by volume (4). This would be a minimum value for the paths used here because the Chesapeake Bay location has appreciable surrounding swamp land, a suggested source of methane (5).

RESULTS

There are available a total of 37 measurement runs, which were obtained on 27 different days. The data from these runs are given in Table 1 which includes information on the precipitable (ppt) water content (column 2) and the transmission per kilometer (T/km) at 0.67μ (column 4) as measured with the telephotometer. In some cases of thick haze or fog the transmission changed during a run. In these cases the transmissions before and after the run were known and are given in column 4 of Table 1. The median value was used for normalizing the data. The values of the coefficients listed in Table 1 for 1.68 and 2.27μ contain corrections for water vapor and methane absorption within the bandpass of the filter. The contributions due to Rayleigh scattering are included in the tabulated data and are listed separately at the end in case the reader desires to eliminate this component from the data. A majority of the runs were made using the 5.5-km path, the long path being used from Oct. 26 through Nov. 30 only. The data corrected for water vapor and methane absorption, and including the Rayleigh contribution, are shown plotted as scattering coefficient vs wavelength in Figs. 3 through 8. For convenience, the curves were grouped as much as possible according to slope. For example, all curves in Fig. 3 are rather flat in the infrared. The lower three curves have increasingly steeper slopes in the visible region. The slope of the bottom curve approaches the slope of a Rayleigh scattering distribution below 0.53μ and has a flat portion which extends into the green. This behavior indicates an average particle size for which the scattering is almost independent of wavelength or, in other words, indicates that the particles are larger than the wavelength of the radiation.

Table 1

Scattering Coefficients at Ten Wavelengths, Including Contributions Due to Rayleigh Scattering by Air Molecules
(Values in the Last Two Columns Include Corrections for Water Vapor and Methane Absorption)

Date	ppt, H_2O (cm)	RH (%)	T/km (at 0.67μ)	0.40μ	0.43μ	0.46μ	0.47μ	0.56μ	0.67μ	0.78μ	1.04μ	1.68μ	2.27μ
April 8	3.3	40	0.88	0.24	0.225	0.190	0.175	0.170	0.130	0.115	0.122	0.065	0.070
9	7.1	42	0.92	0.134	0.112	0.105	0.105	0.075	0.084	0.087	0.084	0.019	0.027
13	2.9	70	0.90	0.24	0.210	0.180	0.185	0.145	0.105	0.109	0.096	0.045	0.032
16	4.4	36	0.95	0.140	0.125	0.180	0.093	0.073	0.052	0.034	0.048	0.025	0.000
21	4.6	79	0.86	-	-	0.210	0.200	0.185	0.122	0.112	0.100	0.045	0.034
24	4.5	55	0.85-0.89	0.25	0.23	0.200	0.195	0.170	0.140	0.130	0.125	0.081	0.070
27	7.0	94	0.49*	1.36	1.26	1.17	1.10	0.98	0.71	0.68	0.53	0.38	0.34
28	4.8	97	0.78*	0.405	0.385	0.345	0.34	0.30	0.25	0.245	0.225	0.151	0.144
29 (1100)	5.8	93	0.70*	0.62	0.59	0.55	0.54	0.46	0.35	0.32	0.225	0.102	0.074
29 (1300)	6.1	88	0.78*	0.46	0.43	0.40	0.38	0.31	0.25	0.23	0.169	0.081	0.060
30	4.0	36	0.60	0.69	0.67	0.63	0.64	0.58	0.505	0.48	0.385	0.28	0.26
Sept. 18	3.7	44	0.89	0.210	0.190	0.167	0.170	0.140	0.120	0.110	0.088	0.055	0.062
22	9.8	81	0.79	0.40	0.37	0.32	0.30	0.24	0.23	0.194	0.150	0.093	0.112
29 (0810)	11.0	-	0.78-0.70	0.36	0.345	0.325	0.325	0.305	0.29	0.26	0.245	0.163	0.182
29 (0825)	11.0	-	0.70-0.67	0.49	0.46	0.445	0.44	0.405	0.38	0.34	0.315	0.255	0.24
29 (0850)	11.0	-	0.78-0.73	0.365	0.345	0.33	0.315	0.295	0.28	0.25	0.24	0.181	0.176
29 (0910)	11.0	-	0.65-0.75	0.425	0.40	0.38	0.385	0.36	0.345	0.31	0.30	0.235	0.26
29 (0945)	11.0	-	0.79-0.77	0.335	0.305	0.29	0.285	0.25	0.25	0.22	0.21	0.158	0.176
29 (1030)	11.0	95	0.77	0.33	0.31	0.29	0.285	0.265	0.265	0.235	0.235	0.173	0.204
Oct. 2	7.6	76	0.88	0.22	0.186	0.162	0.171	0.133	0.122	0.105	0.075	0.0405	0.052
26	11.0	56	0.96	0.091	0.066	0.064	0.061	0.039	0.039	0.040	0.040	0.043	0.045
27	11.5	58	0.92	0.165	0.153	0.136	0.133	0.095	0.087	0.078	0.066	0.053	0.048
28	8.0	47	0.95	0.125	0.115	0.100	0.087	0.070	0.056	0.050	0.041	0.023	0.035
29	9.0	59	0.94	0.157	0.137	0.115	0.105	0.072	0.064	0.061	0.051	0.030	0.041
30	15.5	77	0.91	0.25	0.22	0.197	0.184	0.138	0.096	0.091	0.042	0.017	0.024
Nov. 2	7.0	45	0.96	0.078	0.064	0.059	0.052	0.035	0.039	0.027	0.033	0.014	0.023
3	8.0	57	0.95	0.112	0.090	0.093	0.080	0.056	0.047	0.049	0.042	0.040	0.028
4	13.0	49	0.92	0.159	0.127	0.122	0.107	0.007	0.087	0.070	0.064	0.060	0.063
13	14.0	75	0.75						0.29	0.26	0.188	0.132	0.125
20	7.0	58	0.91	0.196	0.174	0.146	0.149	0.118	0.090	0.080	0.066	0.044	0.0455
30	4.2	38	0.95	0.099	0.101	0.085	0.072	0.055	0.056	0.046	0.041	0.031	0.033
Jan. 5	1.8	44	0.86	0.196	0.180	0.171	0.171	0.137	0.145	0.137	0.137	0.101	0.105
13 (1110)	3.7	92	0.60	1.14	1.04	0.97	0.88	0.74	0.51	0.49	0.32	0.182	0.142
13 (1135)	3.7	-	0.58-0.53*	-	1.24	1.16	1.08	0.89	0.58	0.58	0.34	0.200	0.26
13 (1345)	3.7	-	0.58*	1.18	1.10	1.03	0.95	0.80	0.54	0.53	0.32	0.18	0.117
13 (1440)	3.7	92	0.67*	0.94	0.86	0.79	0.75	0.60	0.40	0.37	0.205	0.092	0.061
13 (1520)	3.7	92	0.67*	0.82	0.75	0.70	0.66	0.54	0.40	0.37	0.24	0.148	0.121
Rayleigh				0.045	0.034	0.025	0.023	0.011	0.005	0.003	0.001	-	-

*Obtained from visual estimate of meteorological range.

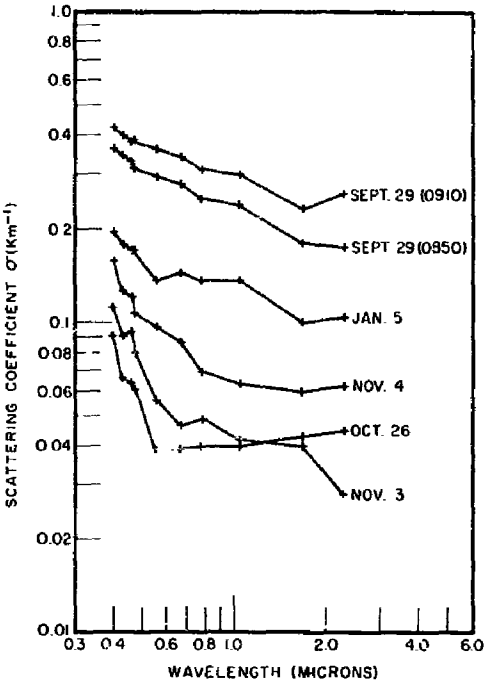

Fig. 3 - Scattering coefficient vs wavelength including Rayleigh scattering. Corrections for water vapor and methane absorption have been made.

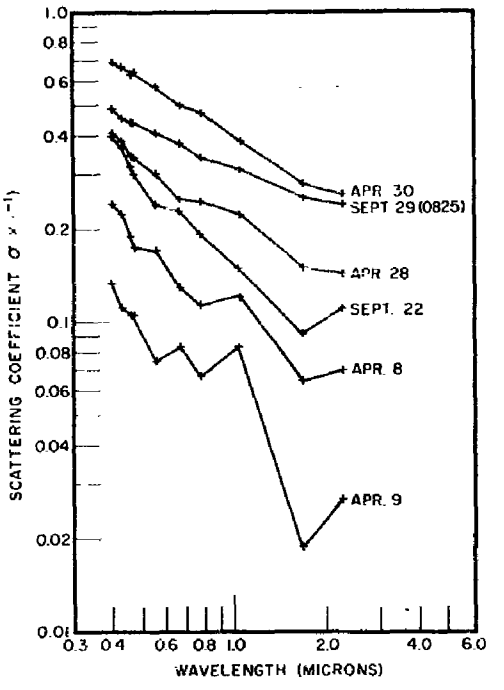

Fig. 4 - Scattering coefficient vs wavelength including Rayleigh scattering. Corrections for water vapor and methane absorption have been made.

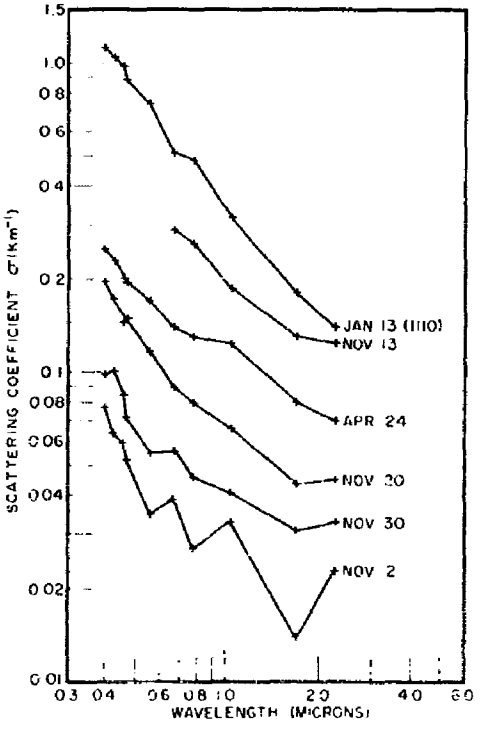

Fig. 5 - Scattering coefficient vs wavelength including Rayleigh scattering. Corrections for water vapor and methane absorption have been made.

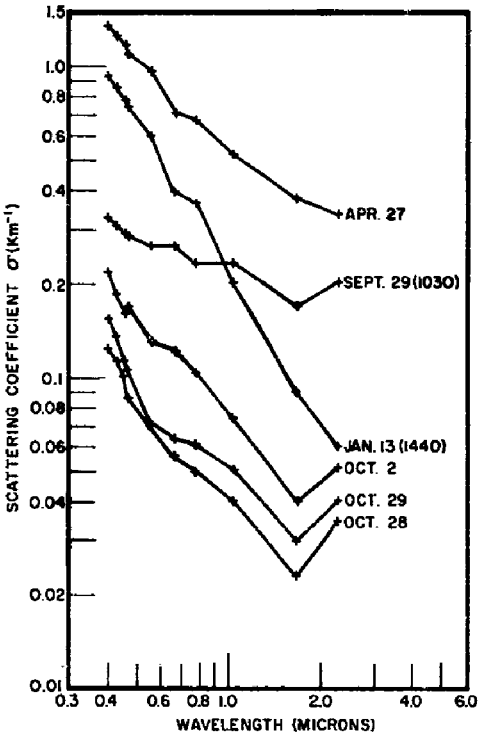

Fig. 6 - Scattering coefficient vs wavelength including Rayleigh scattering. Corrections for water vapor and methane absorption have been made.

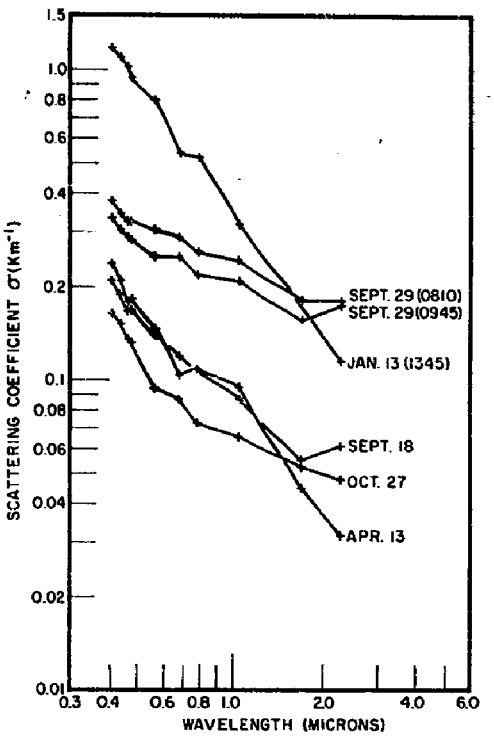

Fig. 7 - Scattering coefficient vs wavelength including Rayleigh scattering. Corrections for water vapor and methane absorption have been made.

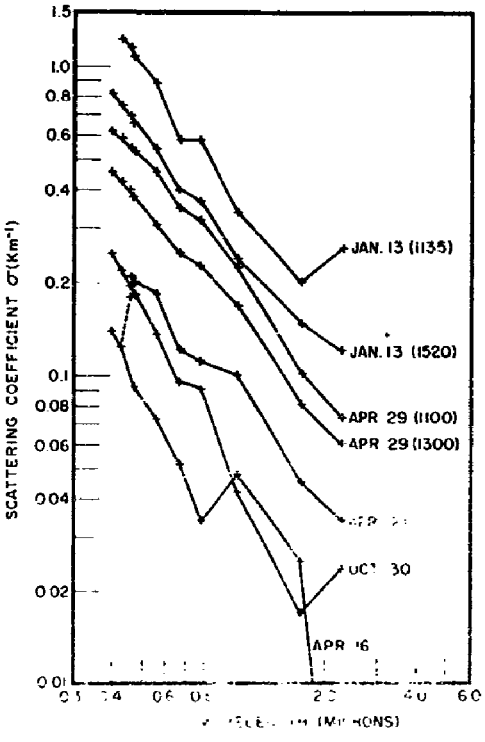

Fig. 8 - Scattering coefficient vs wavelength including Rayleigh scattering. Corrections for water vapor and methane absorption have been made.

DISCUSSION

Scattering Coefficient Curves

Points on the σ vs λ curves were connected by straight lines rather than by drawing a smooth curve of best fit because particle scattering does not necessarily vary monotonically with wavelength. However, most of the deviations of the points from a smooth curve are probably due to accumulated errors in the system, including twinkle, fluctuation of source output, and errors in reading the scope trace. The effect of twinkle is especially noticeable in the data for clear atmospheres, namely, on Apr. 9 (Fig. 4) and Nov. 2 (Fig. 5), even though the average of several readings was taken. The effect was measured on a clear day and found to involve fluctuations of ±6 percent based on the average of 5 readings. This is believed to be the maximum variation due to twinkle.

The relative variation in the point at 2.27μ does not seem to be due entirely to error. In half the cases the value of the coefficient at 2.27μ was greater than that at 1.68μ. Such a slope reversal does not occur this often at any other wavelength. In addition, the data of Yates and Taylor (6) show the same behavior of this point, although with less regularity. The reason for this behavior may involve weak absorption bands in the 2.2-μ region. These appear in the spectral curves of Ref. 6, one of which is reproduced as Fig. 9. At least a small amount of absorption is always present even for a path as short as 1000 feet. This absorption as well as the high measured value of scattering coefficient at 2.27μ are not related to the absolute or the relative humidity, which would seem to rule out water vapor as the causative agent. The only other known absorbing gas in this region is methane (for which an approximate correction has been made). Therefore, if the phenomenon is due to absorption, it is believed that it is not caused by either of the gases for which corrections have already been made. Another possible source of the high scattering coefficient may be some sort of selective scattering.

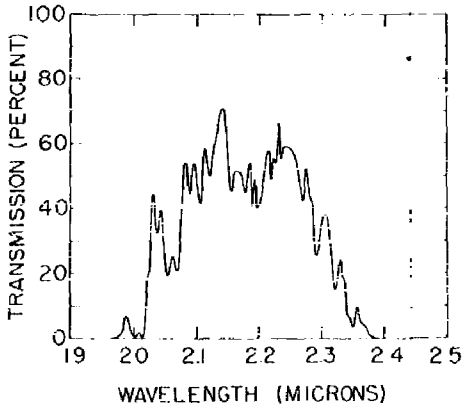

Fig. 9 - Atmospheric transmission for a 16.25-km path as a function of wavelength (from Ref. 6 (showing weak absorption structures in the 2 μ region

The amount of precipitable water contained in the path does not correlate with the scattering, but there is some correlation of scattering with relative humidity (except at the wavelength mentioned above). In Fig. 10 the scattering coefficient at 5600A (0.56μ) is plotted vs relative humidity (RH). For humidities of 70 percent or greater the coefficient depends to some extent on the relative humidity. Below 70 percent RH, however, no dependency exists, which is in agreement with the findings of Junge (7), Wright (8), and others, and bears out Middleton's statement (9) that there is comparatively little change in the radii of the nuclei with changes of relative humidity below about 70 percent. Recently, Boileau (10) and Buma (11) have reported similar findings and in addition have found an apparent discontinuity for relative humidities between 65 and 85 percent. Such a discontinuity is suggested by the present data (Fig. 10) but the evidence is not strong enough to justify it.

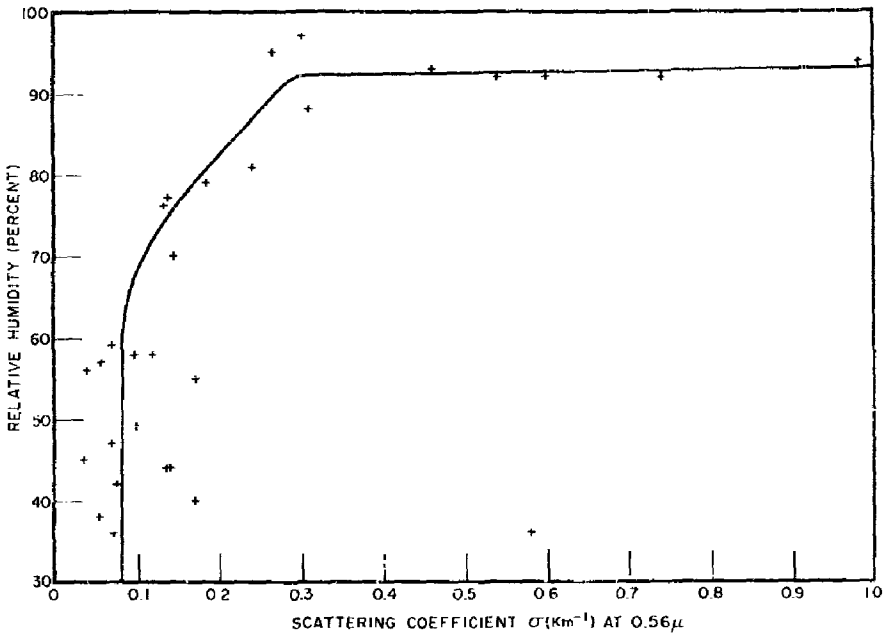

Fig. 10 - Relative humidity vs scattering coefficient at 0.56μ

Coefficient Ratios

One would like to be able to predict the attenuation at a certain wavelength or several wavelengths by means of one or two simple measurements. The meteorological parameters seem to be of little help, but there is some limited correlation between coefficients at various wavelengths. For example, Curcio and Durbin (1) investigated the relationship of the coefficients at three wavelengths in the visible region and obtained average values for the ratios of the coefficients at one wavelength to those at another wavelength. A similar investigation was made using the present data.

In Fig. 11 the attenuation coefficient at 0.47μ is plotted against the coefficient at 0.67μ. The line of best fit would have a slope of +0.97 but a line of slope +1 has been fitted to the data for convenience. This curve gives an average relationship of $\sigma_{0.47} = 1.5\sigma_{0.67}$. This compares favorably with the value of 1.54 obtained by Curcio and Durbin.

In Fig. 12 the attenuation coefficient at 0.56μ is plotted vs the attenuation coefficient at 0.67μ, and by fitting the data with a line of +1 slope, which is within 4% of the slope of the best-fit line, the relation derived is $\sigma_{0.56} = 1.2\sigma_{0.67}$. Curcio and Durbin used 0.535μ instead of 0.56μ, so no direct comparison can be made with their value of 1.32.

A similar plot, Fig. 13, was made of the coefficients in the blue against those in the green resulting in a ratio of $\sigma_{0.47} = 1.25\sigma_{0.56}$. The degree of correlation of coefficients at two different wavelengths depends on the closeness of the wavelengths. For example, when an attempt was made to plot coefficients in the red vs those in the infrared, a rather large spreading of the points resulted, as shown in Figs. 14 and 15 (compare with Figs. 11 to 13). A best-fit line was not applied to Fig. 15 due to the wide spread in the data. This spread is no doubt caused by the change in slope between visible and infrared regions and the fact that this change occurs only part of the time. On the basis of existing data there seems to be little hope of reliably predicting infrared scattering attenuation from a knowledge of the attenuation in the visible. The difficulty is illustrated very pointedly in Fig. 6 by the two curves of Sept. 29 and Jan. 13 which cross at about 1μ.

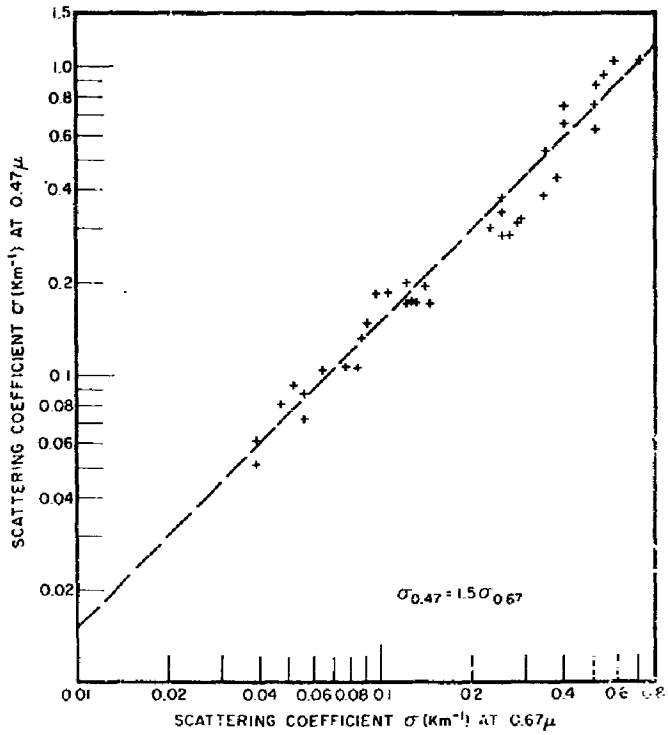

Fig. 11 - Scattering coefficient at 0.47μ vs scattering coefficient at 0.67μ (data from Table 1)

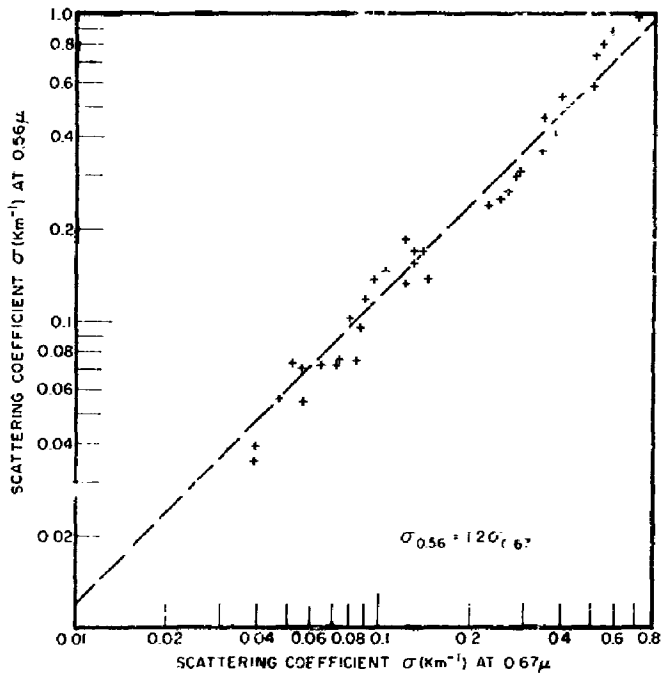

Fig. 12 - Scattering coefficient at 0.56μ vs scattering coefficient at 0.67μ (data from Table 1)

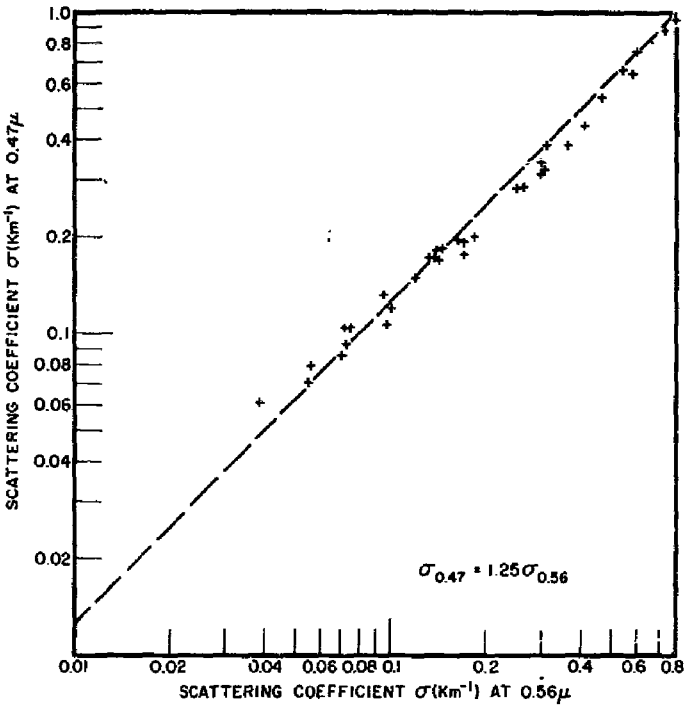

Fig. 13 - Scattering coefficient at 0.47μ vs scattering coefficient at 0.56μ (data from Table 1)

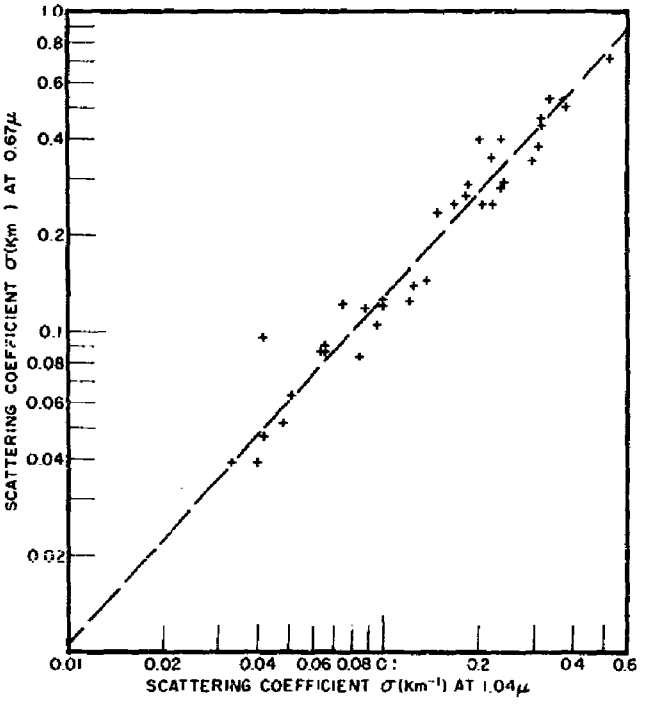

Fig. 14 - Scattering coefficient at 0.67μ vs scattering coefficient at 1.04μ (data from Table 1)

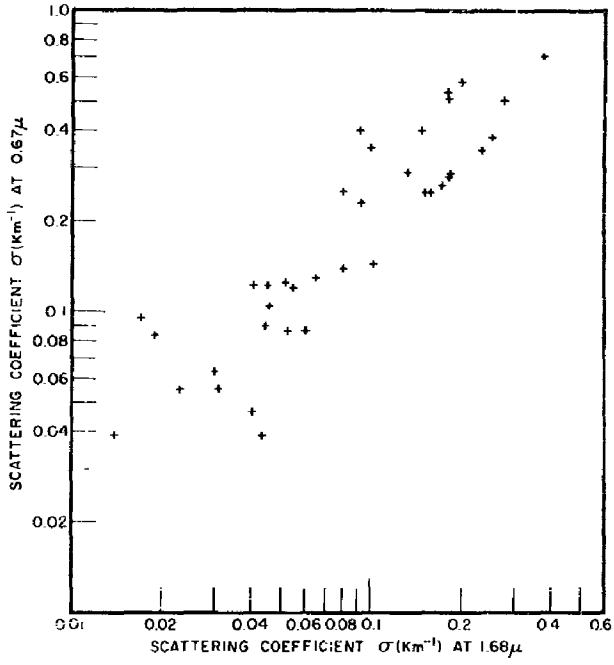

Fig. 15 - Scattering coefficient at 0.67μ vs scattering coefficient at 1.68μ (data from Table 1)

A discussion of these results in relation to estimated particle-size distributions is contained in an NRL report (12) and will not be discussed in detail here. Suffice it to say that, in general, the aerosol on any particular day behaves, insofar as the variations of σ with λ is concerned, like a two-component composite distribution, the main component being described by a Junge distribution of the form $dN/d \log r = Cr^{-n}$ and the other either by a distribution similar to that of aerosols found in maritime air, or by a relatively monodisperse distribution contained in a narrow radius interval.

ACKNOWLEDGMENT

The authors wish to thank Dr. L. F. Drummeter for his guidance and encouragement.

REFERENCES

1. Curcio, J.A., and Durbin, K.A., "Atmospheric Transmission in the Visible Region," NRL Report 5368, Oct. 1959

2. Passman, S., and Larmore, L., "Correction to Atmospheric Transmission Tab (Unclassified), IRIS Proc. 1 (No. 2):15-17, Dec. 1956, Classified Symposium

3. Migeotte, M.V., "On the Presence of Atmospheric Gases from Infrared Telluric Bands," in "The Atmospheres of the Earth and Planets," Kuiper, G.P., ed., Chicago: U. of Chicago Press, 1949

4. Miller, L.E., "Atmospheric Composition," in "Handbook of Geophysics for Air Force Designers," AFCRC, 1957

5. Strong, J., Physics Today, 4(No. 4):14 (1951)

6. Yates, H.W., and Taylor, J.H., "Infrared Transmission of the Atmosphere," NRL Report 5453, June 1960

7. Junge, C., "Übersättigungsmessungen an atmosphärischen Kondensationskernen," Gerlands Beitr. zur Geophys. 46:108-129 (1935)

8. Wright, H.L., "Atmospheric Opacity at Valentia," Q.J. 66:66-77 (1940)

9. Middleton, W.E.K., "Vision Through the Atmosphere," Toronto: U. of Toronto Press, 1952

10. Boileau, A.R., "Correlation between Measured Path Function and Relative Humidity," SIO Reference 59-5, Scripps Institution of Oceanography, U. of California, Feb. 1, 1959

11. Buma, T.J., "A Statistical Study of the Relationship between Visibility and Relative Humidity at Leeuwarden," Bull. Am. Meteorol. Soc. 41:357 (1960)

12. Curcio, J.A., Knestrick, G.L., and Cosden, T.H., "Atmospheric Scattering in the Visible and Infrared," NRL Report 5567, Jan. 1961

* * *

UNCLASSIFIED

Naval Research Laboratory. Report 5648.
ATMOSPHERIC ATTENUATION COEFFICIENTS IN THE VISIBLE AND INFRARED REGIONS by
G. L. Knestrick, T. H. Cosden, and J. A. Curcio.
12 pp. & figs., August 8, 1961.

Atmospheric spectral attenuation coefficients have been measured in ten narrow wavelength bands between 0.4 and 2.3 microns for a variety of weather conditions using two overwater, sea-level paths of 5.5 km and 16.3 km. The wavelengths bands were chosen so as to avoid molecular absorption and were isolated by interference filters. A 60-inch-diameter, high-intensity source and a 24-inch-diameter, narrow-field receiver were combined to yield relative scattering attenuation coefficients ( ) as a function of wavelength ( ). These were

UNCLASSIFIED (Over)

1. Atmosphere – Absorptive properties
2. Light – Attenuation
3. Infrared waves – x Attenuation

I. Knestrick, G. L.
II. Cosden, T. H.
III. Curcio, J. A.

UNCLASSIFIED

Naval Research Laboratory. Report 5648.
ATMOSPHERIC ATTENUATION COEFFICIENTS IN THE VISIBLE AND INFRARED REGIONS by
G. L. Knestrick, T. H. Cosden, and J. A. Curcio.
12 pp. & figs., August 8, 1961.

Atmospheric spectral attenuation coefficients have been measured in ten narrow wavelength bands between 0.4 and 2.3 microns for a variety of weather conditions using two overwater, sea-level paths of 5.5 km and 16.3 km. The wavelengths bands were chosen so as to avoid molecular absorption and were isolated by interference filters. A 60-inch-diameter, high-intensity source and a 24-inch-diameter, narrow-field receiver were combined to yield relative scattering attenuation coefficients (σ) as a function of wavelength (λ). These were

UNCLASSIFIED (Over)

1. Atmosphere – Absorptive properties
2. Light – Attenuation
3. Infrared waves – x Attenuation

I. Knestrick, G. L.
II. Cosden, T. H.
III. Curcio, J. A.

UNCLASSIFIED

Naval Research Laboratory. Report 5648.
ATMOSPHERIC ATTENUATION COEFFICIENTS IN THE VISIBLE AND INFRARED REGIONS by
G. L. Knestrick, T. H. Cosden, and J. A. Curcio.
12 pp. & figs., August 8, 1961.

Atmospheric spectral attenuation coefficients have been measured in ten narrow wavelength bands between 0.4 and 2.3 microns for a variety of weather conditions using two overwater, sea-level paths of 5.5 km and 16.3 km. The wavelengths bands were chosen so as to avoid molecular absorption and were isolated by interference filters. A 60-inch-diameter, high-intensity source and a 24-inch-diameter, narrow-field receiver were combined to yield relative scattering attenuation coefficients (σ) as a function of wavelength (λ). These were

UNCLASSIFIED (Over)

1. Atmosphere – Absorptive properties
2. Light – Attenuation
3. Infrared waves – x Attenuation

I. Knestrick, G. L.
II. Cosden, T. H.
III. Curcio, J. A.

UNCLASSIFIED

Naval Research Laboratory. Report 5648.
ATMOSPHERIC ATTENUATION COEFFICIENTS IN THE VISIBLE AND INFRARED REGIONS by
G. L. Knestrick, T. H. Cosden, and J. A. Curcio.
12 pp. & figs., August 8, 1961.

Atmospheric spectral attenuation coefficients have been measured in ten narrow wavelength bands between 0.4 and 2.3 microns for a variety of weather conditions using two overwater, sea-level paths of 5.5 km and 16.3 km. The wavelengths bands were chosen so as to avoid molecular absorption and were isolated by interference filters. A 60-inch-diameter, high-intensity source and a 24-inch-diameter, narrow-field receiver were combined to yield relative scattering attenuation coefficients (σ) as a function of wavelength ( ). These were

UNCLASSIFIED (Over)

1. Atmosphere – Absorptive properties
2. Light – Attenuation
3. Infrared waves – x Attenuation

I. Knestrick, G. L.
II. Cosden, T. H.
III. Curcio, J. A.

then scaled using values obtained at one wavelength with a visual telephotom-
eter. Log σ vs log λ curves show a wide range of slopes and shapes, with a
tendency toward less slope in the infrared (indicating that σ is becoming inde-
pendent of λ in the infrared). Some correlation with relative humidity was
found for relative humidities greater than 70 percent. The anomalous slope
reversal between 1.68 and 2.27 μ is discussed, and a possible explanation for
the reversal is given as selective scattering by the aerosol at these
wavelengths.

UNCLASSIFIED

UNCLASSIFIED

then scaled using values obtained at one wavelength with a visual telephotom-
eter. Log σ vs log λ curves show a wide range of slopes and shapes, with a
tendency toward less slope in the infrared (indicating that σ is becoming inde-
pendent of λ in the infrared). Some correlation with relative humidity was
found for relative humidities greater than 70 percent. The anomalous slope
reversal between 1.68 and 2.27 μ is discussed, and a possible explanation for
the reversal is given as selective scattering by the aerosol at these
wavelengths.

UNCLASSIFIED

UNCLASSIFIED

then scaled using values obtained at one wavelength with a visual telephotom-
eter. Log σ vs log λ curves show a wide range of slopes and shapes, with a
tendency toward less slope in the infrared (indicating that σ is becoming inde-
pendent of λ in the infrared). Some correlation with relative humidity was
found for relative humidities greater than 70 percent. The anomalous slope
reversal between 1.68 and 2.27 μ is discussed, and a possible explanation for
the reversal is given as selective scattering by the aerosol at these
wavelengths.

UNCLASSIFIED

UNCLASSIFIED